Asian megacity heat stress under future climate scenarios: impact of air-conditioning feedback

It is advisable to refer to the publisher's version if you intend to cite from the work. See Guidance on citing.

To link to this article DOI: http://dx.doi.org/10.1088/2515-7620/ab6933

the End User Agreement.

www.reading.ac.uk/centaur

CentAUR

Central Archive at the University of Reading

Reading's research outputs online

PAPER • OPEN ACCESS

Asian megacity heat stress under future climate scenarios: impact of air-conditioning feedback

View the article online for updates and enhancements.

Environmental Research Communications

PAPER

Asian megacity heat stress under future climate scenarios: impact of air-conditioning feedback

Yuya Takane[1,2] , **Yukitaka Ohashi**[3] , **C Sue B Grimmond**[2] , **Masayuki Hara**[4] **and Yukihiro Kikegawa**[5]

1   Environmental Management Research Institute, National Institute of Advanced Industrial Science and Technology, Tsukuba, Ibaraki, Japan
2   Department of Meteorology, University of Reading, Reading, United Kingdom
3   Faculty of Biosphere-Geosphere Science, Okayama University of Science, Okayama, Japan
4   Center for Environmental Science in Saitama, Kazo, Saitama, Japan
5   School of Science and Engineering, Meisei University, Hino, Tokyo, Japan

E-mail: takane@aist.go.jp **and** y.takane@reading.ac.uk

Abstract

Future heat stress under six future global warming (ΔT_{GW}) scenarios (IPCC RCP8.5) in an Asian megacity (Osaka) is estimated using a regional climate model with an urban canopy and air-conditioning (AC). An urban heat 'stress' island is projected in all six scenarios ($\Delta T_{GW} = +0.5$ to $+3.0\,^\circ$C in $0.5\,^\circ$C steps). Under $\Delta T_{GW} = +3.0\,^\circ$C conditions, people outdoors experience 'extreme' heat stress, which could result in dangerously high increases in human body core temperature. AC-induced feedback increases heat stress roughly linearly as ΔT_{GW} increases, reaching $0.6\,^\circ$C (or 12% of the heat stress increase). As this increase is similar to current possible heat island mitigation techniques, this feedback needs to be considered in urban climate projections, especially where AC use is large.

Abbreviations and notation used

AC	Air-conditioning
AC→FB	Simulation with AC feedback (FB)
AC≠FB	Simulation without AC FB (no-$Q_{F, AC}$)
BEP+BEM	Building effect parameterisation and building energy model
C	Commercial and office
C_g	Sensible heat flux from the globe surface (W m^{-2})
c_P	Specific heat at constant pressure (J K^{-1} kg^{-1})
CM-BEM	Urban canopy model and building energy model
CMIP	Climate model intercomparison project
COP	Coefficient of performance
COST	Cooperation in science and technical development
D	Diameter of the globe (m)
FB	Feedback
GCM	Global climate model
GHG	Greenhouse gas
GIAJ	Geospatial Information Authority of Japan
GIS	Geospatial information system
IPCC	Intergovernmental Panel for Climate Change

JMA	Japan Meteorological Agency
LULC	Land use and land cover
MGDSST	Merged satellite and in site global daily sea surface temperature
MYJ	Mellor-Yamada-Janjic
NCEP-NCAR	National Center for Environmental Prediction—National Center for Atmospheric Research
PGW	Pseudo global warming
Q_F	Anthropogenic heat flux (W m^{-2})
$Q_{F,AC}$	Q_F from AC use (W m^{-2})
RCM	Regional climate model
RCP	Representative concentration pathway
Re	Reynolds number (−)
R_g	Longwave radiation emitted from a globe surface averaged by surface area (W m^{-2})
Rr	Residential area with predominantly concrete fireproof apartments
RRTMG	Updated rapid radiation transfer model
Rw	Residential area with predominantly detached wooden dwellings
S_0	Incoming shortwave radiation (W m^{-2})
SLUCM	Single-layer UCM
SOLWEIG	Solar and longwave environmental irradiance geometry-model
T_g	Black globe temperature (°C)
TEB + BEM	Town energy balance and building energy model
T_{mrt}	Mean radiant temperature (°C)
U	Wind speed (m s^{-1})
UCM	Urban canopy model
UCLEM	Urban climate and energy model
UTCI	universal thermal climate index
ν	Kinematic viscosity of air (m^2 s^{-1})
WBGT	Wet-bulb globe temperature
WRF	Weather research and forecasting
WSM3	WRF single-moment three-class
γ	Viscosity coefficient of air (Pa s^{-1})
ΔT_{GW}	Global warming (°C)
$\Delta UTCI_{AC \to FB}$	UTCI difference between the current and future climate for AC→FB
$\Delta UTCI_{AC \neq FB}$	UTCI difference between the current and future climate for AC≠FB
$\delta UTCI_{AC \to FB}$	UTCI difference between the AC →FB and the AC≠FB
ε_g	Emissivity of the globe thermometer (−)
ε_h	Emissivity of human clothing (−)
λ	Thermal conductivity of air (W m^{-1} K^{-1})

1. Introduction

In 2018, Japan had the second hottest July on record (since 1883, Japan Meteorological Agency (JMA) official home page: https://www.data.jma.go.jp), with a mean monthly temperature in Osaka 1.63 °C higher than the 11 year (July 2000–2010) mean. These elevated temperatures resulted in the highest on record hospitalisations (54,220) and heat stroke deaths (133) (Ministry of Internal Affairs and Communications, Japan 2018). This period was designated a 'heat wave natural disaster' (Nikkei 2018), similar to disasters from typhoons, heavy rainfall and snowfall, and floods.

Heat waves are expected to become more common and more intense with greenhouse gas (GHG)–induced global warming (e.g. IPCC 2013), exacerbated in cities by the urban heat island effect (e.g. IPCC 2014). With cities being home to more than 66% of the population by 2050 (United Nations 2014), the impact of urban

climate on public health and energy supply/demand is critical. Already 30% of the world's population are exposed to deadly heat thresholds on at least 20 days per year, and this may increase to ∼74% by 2100 if GHG emissions increase (Mora *et al* 2017).

To prepare for future heat waves, it is critical to understand how urban heat stress will change and to identify potential feedbacks from GHG-induced global warming and human activities. Although future urban air temperatures have been explored both globally and locally (e.g. Adachi *et al* 2012, Kusaka *et al* 2012, Kusaka *et al* 2016, Hamdi *et al* 2014, Grossman-Clarke *et al* 2016, Conlon *et al* 2016, Krayenhoff *et al* 2018, Tewari *et al* 2019, Darmanto *et al* 2019, Takane *et al* 2019, Lipson *et al* 2019), few studies have examined the impact on human heat stress in cities. As global climate model (GCM) simulations (e.g. Delworth *et al* 1999, Willett and Sherwood 2012, Coffel *et al* 2018) still do not resolve most cities, it is difficult to predict urban heat stress.

A GCM (1° horizontal resolution) with an Urban Canopy Model (UCM) calculated the wet-bulb globe temperature (WBGT) heat stress metric (Fischer *et al* 2012), but this is too coarse for within-city variations. High resolution simulations using dynamical downscaling with a regional climate model (RCM) have allowed heat stress studies at 20 km (e.g. Mediterranean Diffenbaugh *et al* 2007) and 3 km resolution (e.g. Japan Kusaka *et al* 2012). Higher-resolution (a few kilometres) heat stress studies have addressed cities in Asia (Takane *et al* 2015, Suzuki-Parker and Kusaka 2015, 2016, Yang *et al* 2016, Kikumoto *et al* 2016, Doan *et al* 2016, Doan and Kusaka 2018, Yamamoto *et al* 2018), Europe (Altinsoy and Yildirim 2014), North America (Oleson *et al* 2015), and Oceania (Argüeso *et al* 2015).

In Japan, WBGT is the official thermal stress index (since 2006, Ministry of the Environment, http://www.wbgt.env.go.jp/en/). Although it is correlated with both the number of heatstroke patients (heat disorder risk) (Ohashi *et al* 2014, Yamamoto *et al* 2018) and excess deaths (Takaya *et al* 2014), it does not have a clear relationship with human physiological responses (Yaglou and Minard 1957). However, the Universal Thermal Climate Index (UTCI) (Fiala *et al* 2012, Błażejczyk *et al* 2013) is derived from human physiology experiments (Bröde *et al* 2012a), physiological modelling, meteorology, and climatology (Błażejczyk *et al* 2013). It has been applied in a range of climate conditions (Błażejczyk *et al* 2012, Schreier *et al* 2013, Błażejczyk *et al* 2014) and applications (Fiala *et al* 2010, 2012). Heat stress also depends on micro-scale variations in urban morphology (e.g. shading) and differences in individuals (e.g. age, size, movement, activity). Hence, local-scale grid globe temperatures do not capture micro-scale variability or range of values from shading, but rather the mean for the area (section 2.3). However, grid mean heat stress can indicate the most dangerous conditions that outdoor workers will be exposed to, helping risk assessments for human health.
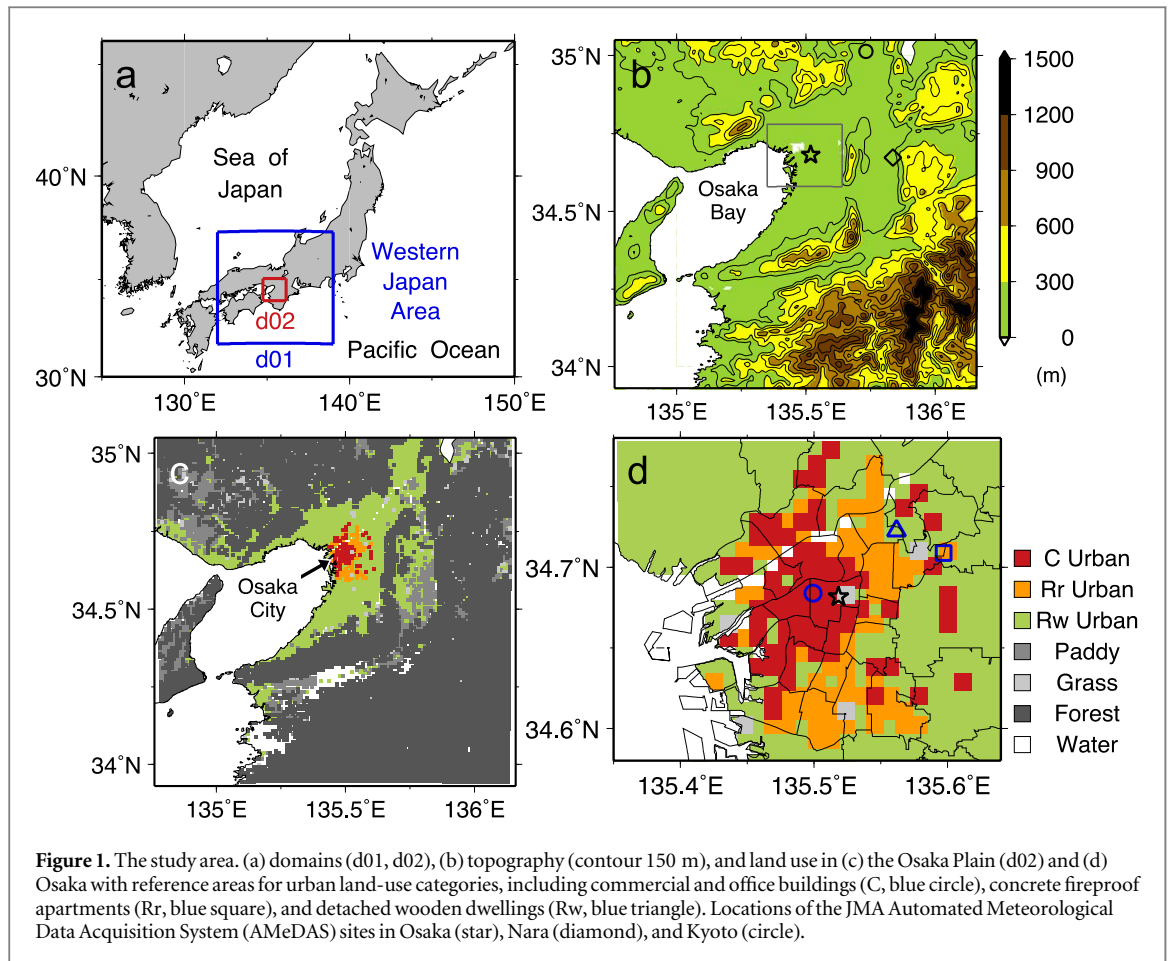
Japan's many megacities have high population densities (e.g. Tokyo and Osaka) where people are exposed to both high temperature and humidity. Hence, there is high risk of both heat stress and heatstroke during heat waves. Additionally, Japanese cities already use air-conditioning (AC) extensively with the associated release of anthropogenic heat (Q_F, i.e. $Q_{F, AC}$). With warmer temperatures, $Q_{F, AC}$ can increase causing a positive feedback leading to additional urban warming and energy consumption (e.g. Ashie *et al* 1999, Kikegawa *et al* 2003, Sailor 2011, Li *et al* 2014, Kikegawa *et al* 2014, Salamanca *et al* 2014, Takane *et al* 2017, Ginzhurg and Demchenko 2019, Takane *et al* 2019). In Osaka, this positive feedback is predicted to cause 0.6 °C additional warming in early morning August temperatures (based on a four-GCM ensemble for +3.0 °C (cf to current) global warming scenario, ∼2070 s). Given this is a similar size to differences or uncertainties within GHG emission scenarios, RCMs, and urban planning scenarios, this feedback need to be considered (Takane *et al* 2019).

Our objectives are to predict the impacts on heat stress from future climate at 1-km horizontal resolution, considering the feedbacks from $Q_{F, AC}$. We focus on Osaka, the second largest city in Japan (figure 1), as it has experienced the hottest mean summer temperatures in Japan in the past 30 years (Takane *et al* 2013). Osaka's humid climate results in greater daytime urban heat island intensities than cities with drier climates (Zhao *et al* 2014). Moreover Osaka, already a major tourist destination, will host the 2025 World Expo, thus thermal stress is of concern to both local citizens and global visitors.

2. Methods

In this study we indicate differences between the current and future climate as Δ (e.g., ΔT); and with ($\rightarrow$) and without ($\neq$) air-conditioning (AC) feedback (FB) as δ (e.g., $\delta UTCI$ is the UTCI difference between AC$\rightarrow$FB and AC$\neq$FB).

Feedback from AC use ($\delta UTCI_{AC \rightarrow FB}$) on future urban climates under future global warming scenarios (ΔT_{GW}) and changes in $\delta UTCI_{AC \rightarrow FB}$ related to ΔT_{GW} are estimated. All methods (numerical model, model setup, and climate projections) are as in Takane *et al* (2019), except for the UTCI and WBGT calculations. The latter are described within the Supplemental Materials.

Figure 1. The study area. (a) domains (d01, d02), (b) topography (contour 150 m), and land use in (c) the Osaka Plain (d02) and (d) Osaka with reference areas for urban land-use categories, including commercial and office buildings (C, blue circle), concrete fireproof apartments (Rr, blue square), and detached wooden dwellings (Rw, blue triangle). Locations of the JMA Automated Meteorological Data Acquisition System (AMeDAS) sites in Osaka (star), Nara (diamond), and Kyoto (circle).
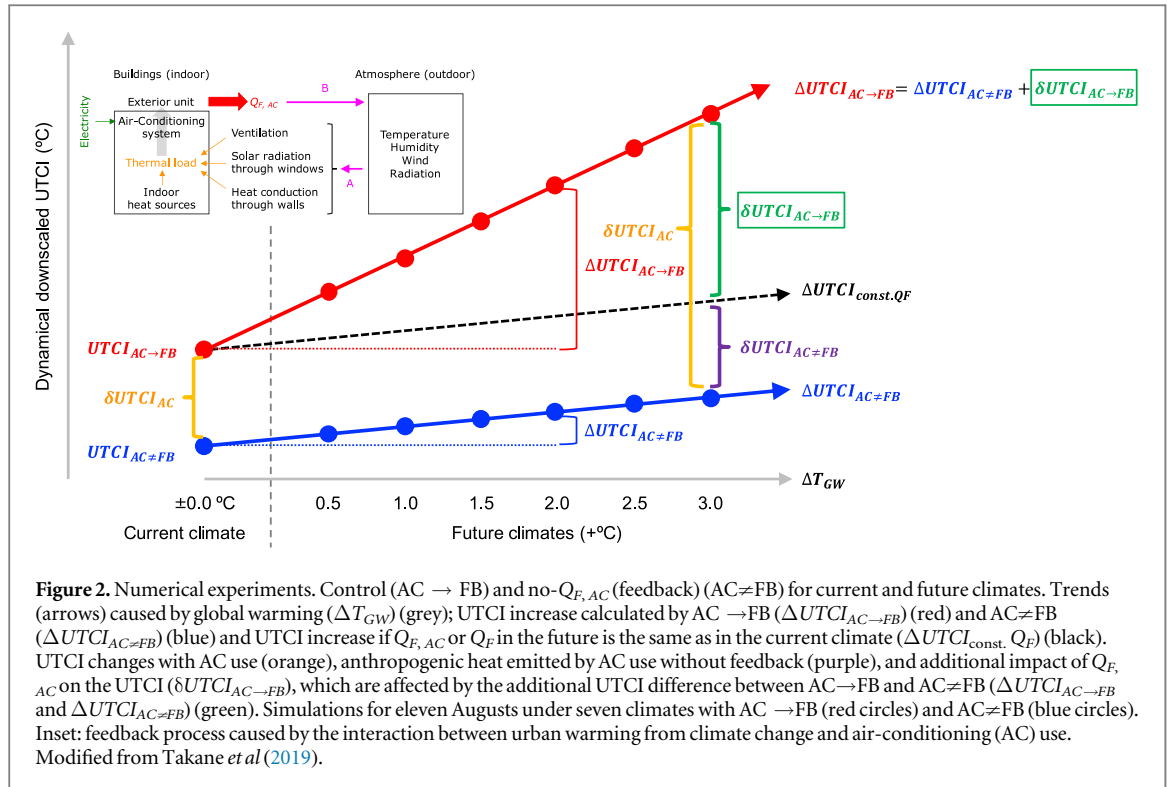
2.1. Model settings

Following Takane *et al* (2017, 2019) dynamic downscaling is undertaken using the Advanced Research WRF model (ver. 3.5.1) (Skamarock *et al* 2008) with model parameters as indicated in table S1 (Supplemental Material) and the following physics schemes: updated Rapid Radiation Transfer Model (RRTMG) short-wave and longwave radiation (Iacono *et al* 2008); WRF single-moment three-class (WSM3) cloud microphysics (Dudhia 1989, Hong *et al* 2004); Mellor–Yamada–Janjic (MYJ) atmospheric boundary-layer (Mellor and Yamada 1982, Janjic 1994, 2002); Noah land surface model (Chen and Dudhia 2001); and BEP +BEM urban canopy parameterisation (Martilli *et al* 2002, Salamanca and Martilli 2010, Salamanca *et al* 2010). At each time step, $Q_{F, AC}$ is calculated from electricity consumption using BEP+BEM for each 1 km grid. Summertime near surface air temperature and AC electricity consumption skill have been assessed for Osaka considering diurnal and spatial variations (Takane *et al* 2017, 2019).

Two model domains (d01 and d02, figure 1(a)) have 126 × 126 grid points (*x*, *y*) at 5- and 1-km resolution, respectively. Vertically, the 35 sigma levels go up to 50 hPa. Land use, land cover (LULC) and topography data are from the Geospatial Information Authority of Japan (GIAJ). In d02, the GIAJ LULC and Osaka geographical information system (GIS) building footprint (polygon) data (figures 1(c), (d)) are used to classify the urban grids into (i) commercial and business (C); and residential with predominantly (ii) concrete fireproof apartments (Rr) or (iii) detached wooden dwellings (Rw). In d01, all urban areas are assumed to be Rw.

Initial and boundary conditions use NCEP–NCAR (National Centers for Environmental Prediction–National for Atmospheric Research) reanalysis (Kalnay *et al* 1996) and merged satellite - *in situ* global daily sea surface temperature (MGDSST) (Kurihara *et al* 2006) data. As 11 Augusts are sufficient for climatological impacts and effects to be considered (Takane *et al* 2017, 2019), the time integration for each year is from 00:00 UTC July 27 to September 1, with model spin-up. The 2000–2010 period is treated as the control simulation (case AC →FB) (figure 2, red arrow).

The no-$Q_{F, AC}$ (feedback) simulation (case AC≠FB) differs from the control simulation as $Q_{F, AC}$ is assumed to be 0 W m^{-2} (figure 2, blue arrow); i.e. the larger difference in UTCI between AC≠FB and AC→FB is the $Q_{F, AC}$ feedback effect ($\delta UTCI_{AC→FB}$). Additionally, six future climates are simulated (section 2.2). We estimate $\delta UTCI_{AC→FB}$ from $\Delta UTCI_{AC→FB} - \Delta UTCI_{AC≠FB}$ (figure 2), with $\delta UTCI_{AC→FB}$ for the current climate being 0 °C as we assume no long-term climate change (decades) (i.e., no increase in forcing temperature, and

Figure 2. Numerical experiments. Control (AC → FB) and no-$Q_{F,AC}$ (feedback) (AC≠FB) for current and future climates. Trends (arrows) caused by global warming (ΔT_{GW}) (grey); UTCI increase calculated by AC →FB ($\Delta UTCI_{AC→FB}$) (red) and AC≠FB ($\Delta UTCI_{AC≠FB}$) (blue) and UTCI increase if $Q_{F,AC}$ or Q_F in the future is the same as in the current climate ($\Delta UTCI_{const.\,Q_F}$) (black). UTCI changes with AC use (orange), anthropogenic heat emitted by AC use without feedback (purple), and additional impact of $Q_{F,AC}$ on the UTCI ($\delta UTCI_{AC→FB}$), which are affected by the additional UTCI difference between AC→FB and AC≠FB ($\Delta UTCI_{AC→FB}$ and $\Delta UTCI_{AC≠FB}$) (green). Simulations for eleven Augusts under seven climates with AC →FB (red circles) and AC≠FB (blue circles). Inset: feedback process caused by the interaction between urban warming from climate change and air-conditioning (AC) use. Modified from Takane *et al* (2019).

$\Delta UTCI_{AC→FB}$ and $\Delta UTCI_{AC≠FB}$ are 0 °C). To determine $\delta UTCI_{AC→FB}$, we assume that all conditions (e.g. urban structures and human activities) remain constant except for background climate change. Although unrealistic, this allows the specific impact of interest to be investigated.

2.2. Climate projection

Six future climates with background temperature increases (global warming with ΔT_{GW} = +0.5, +1.0, +1.5, +2.0, +2.5, and +3.0 °C) relative to the current climate are simulated. The ensemble mean from four global climate models (GCMs) that participated in the Climate Model Intercomparison Project (CMIP5) (Taylor *et al* 2012): CCSM4 (Gent *et al* 2011), CESM1 (CAM5) (Meehl *et al* 2013), GFDL-CM3 (Donner *et al* 2011), and INM-CM4 (Volodin *et al* 2010); simulations for the representative concentration pathway [RCP] 8.5 are used. These are the highest Intergovernmental Panel on Climate Change (IPCC) greenhouse gas emissions scenario.

The climate variables (i.e. wind components, geopotential height, and temperature) differences between the current and future scenarios are estimated (figure 3). For each ΔT_{GW} case, the climate difference for each variable is added to the NCEP–NCAR and MGDSST data (figure 3) but with the relative humidity kept the same as the current climate. Advantages of this regional climate projection (so-called pseudo-global warming (PGW)) method (Kimura and Kitoh 2007, Sato *et al* 2007) is that it bias-corrected (e.g. Xu and Yang 2012, Bruyère *et al* 2014, 2015), widely used (e.g. Hara *et al* 2008, Kawase *et al* 2009, Rasmussen *et al* 2011, Kusaka *et al* 2012, 2016, Doan and Kusaka 2018, Takane *et al* 2019), and a verified (Kawase *et al* 2008, 2009, Yoshikane *et al* 2012) method.

2.3. UTCI calculation

The hourly UTCI is calculated for 11 years for each climate scenario using the Fiala *et al* (2012) human physiology polynomial parameterisation (Bröde *et al* 2012a, Błażejczyk *et al* 2013) as it is computational efficient (e.g. Bröde *et al* 2012b, Błażejczyk *et al* 2013, Provençal *et al* 2016, Ohashi *et al* 2018). It is forced with the near surface air temperature (2-m simulations or 1.5-m observations), relative humidity, black globe temperature (T_g), and wind speed (within the urban canopy layer) (figure 3). The mean radiant temperature (T_{mrt}) is estimated from T_g, air temperature, and wind speed (Kinouchi 2001):

$$\varepsilon_h \sigma (T_{mrt} + 273.15)^4 = C_g + R_g \tag{1}$$

$$R_g = \varepsilon_g \sigma (T_g + 273.15)^4 \tag{2}$$

where C_g is the sensible heat flux from the globe surface (W m^{-2}), R_g is the longwave radiation emitted from the globe surface averaged for the surface area (W m^{-2}), and ε_g and ε_h are the emissivities of the globe thermometer (assumed to be 1.0) and human clothing (0.98), respectively. C_g is a function of globe temperature and air

Figure 3. Calculation flowchart for heat stress metrics under current and future climates.
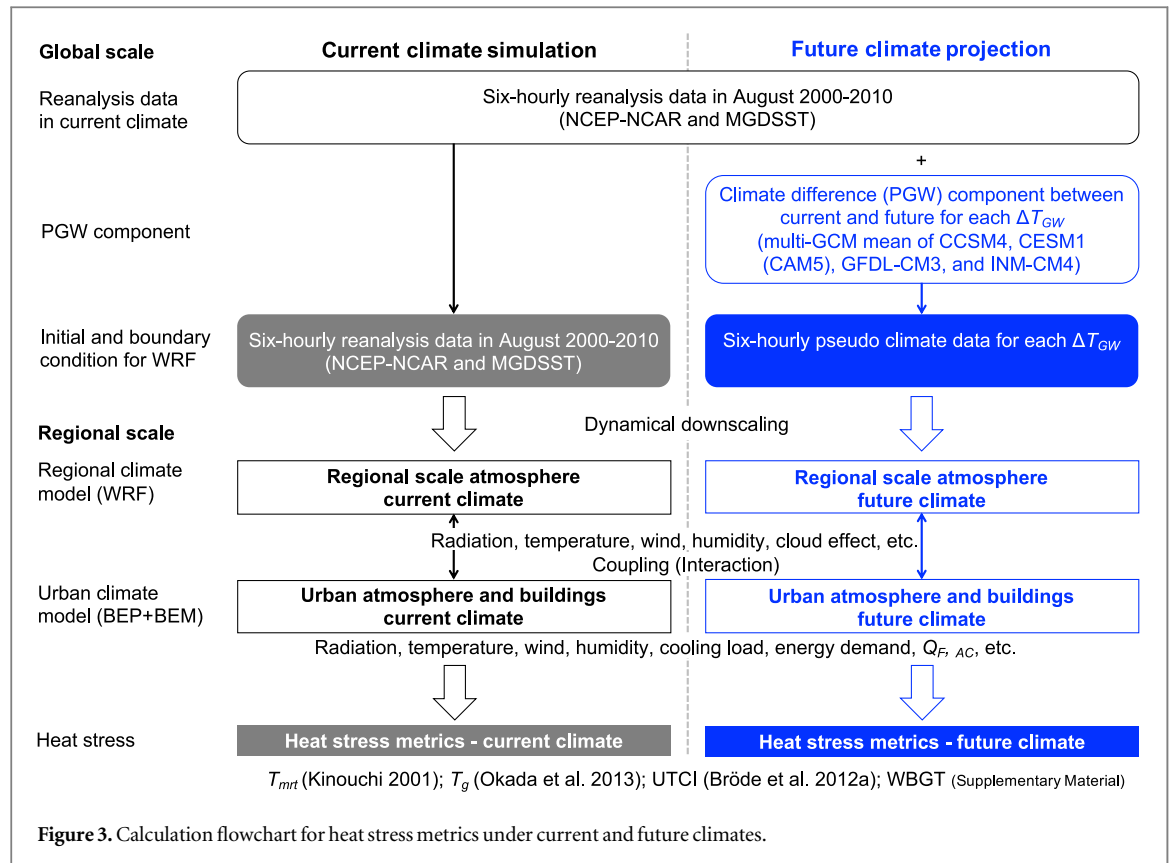
temperature (Yuge 1960):

$$C_g = h_{cg}(T_g - T_a) \tag{3}$$

$$\frac{h_{cg}D}{\lambda} = 2 + 0.55Re^{0.5}\left(\frac{c_p\mu}{\lambda}\right)^{\frac{1}{3}} \quad (10 < \mathrm{Re} < 1.8 \times 10^3) \tag{4}$$

$$\frac{h_{cg}D}{\lambda} = 2 + 0.34Re^{0.566}\left(\frac{c_p\mu}{\lambda}\right)^{\frac{1}{3}} \quad (1.8 \times 10^3 < \mathrm{Re} < 1.5 \times 10^5) \tag{5}$$

where Re is the Reynolds number (UD/ν), U is the wind speed, D the diameter of the globe (=0.15 m), ν is the kinematic viscosity of air (m^2 s^{-1}), γ is the viscosity coefficient of air (Pa s), λ is the thermal conductivity of air (W m^{-1} K^{-1}), and c_p is the specific heat at constant pressure (J K^{-1} kg^{-1}).

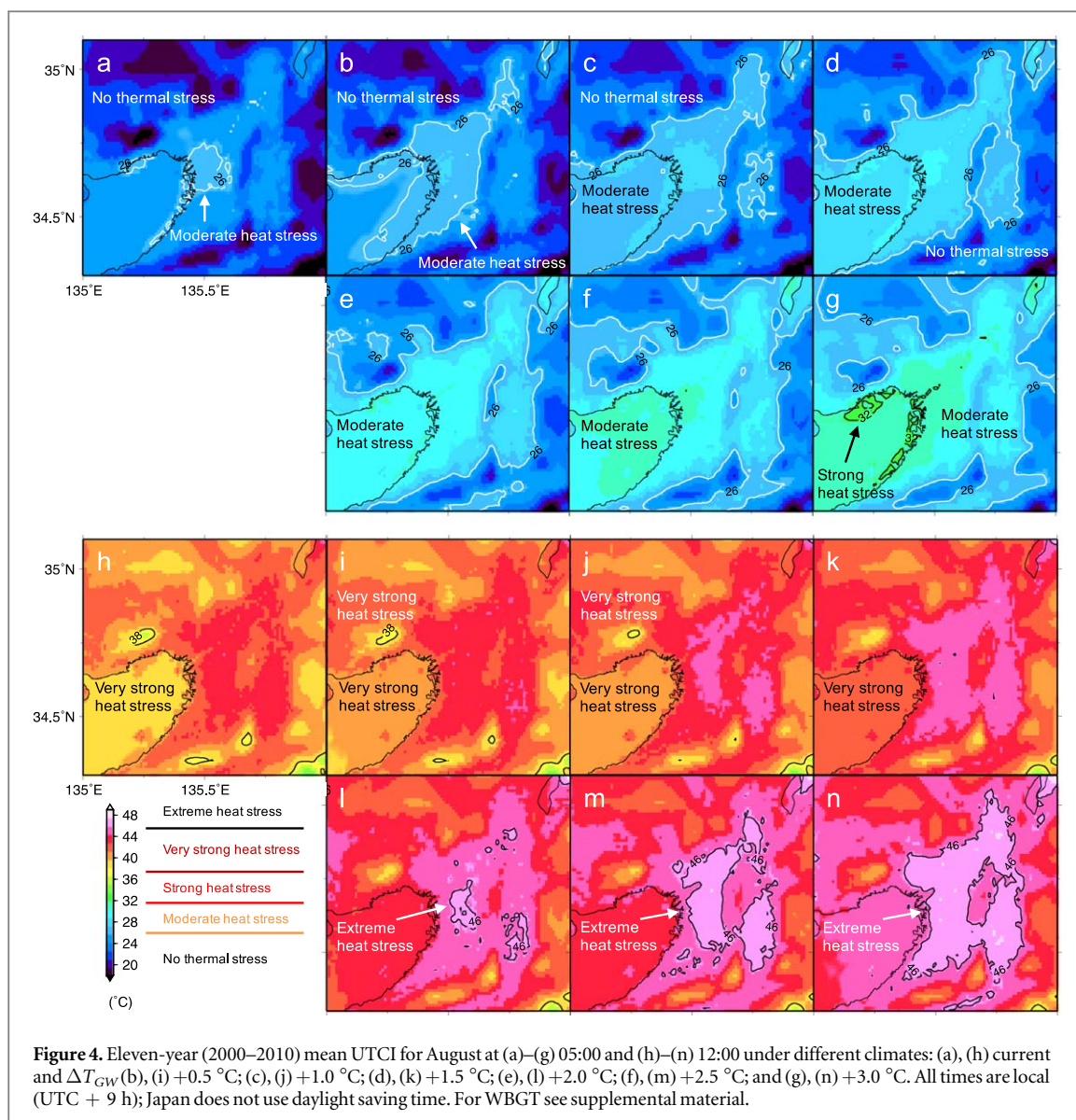T_g is estimated using the (Okada and Kusaka 2013, Okada *et al* 2013) improvement:

$$T_g = \frac{(S_0 - 38.5)}{(0.0217S_0 + 4.35U + 23.5)} + T_a \tag{6}$$

where S_0 is the incoming shortwave radiation (W m^{-2}). Okada *et al* (2013) determined the equation (6) parameters from hourly observations (June-August 2006–2012, all weather conditions) at a Osaka site surrounded by office buildings (RMSE (root mean square error) = 2.15 °C).

The grid average UTCI and WBGT calculated provide information on exposure for outdoor workers allowing risk assessment for human health. Heat stress metrics for within shadow conditions (e.g. Ohashi *et al* 2014) can reduce UTCI by ~8 °C (WBGT by ~1.5 °C) in summer daytime in Tokyo (Honjo *et al* 2018). However, most regional scale heat stress studies use mean radiative conditions (as we do) they allow the regional scale distribution of heat stress or the heat 'stress' island (section 3.1) to be identified, and its change with climate change to be assessed. Regional scale values provide useful initial and/or boundary conditions for higher resolution building resolving models with street level shade and flows around building and trees.

2.4. Verification
The model setup (this section) verificiation is presented in Supplementary material (S1). As the urban charactistics of Osaka (figure 1(d)) do not produce a large difference between the two types of residential area (wooden detached dwellings and fireproof apartments), we only present the results for the area of wooden detached dwellings (hereafter residential) and the commercial and office buildings (commercial).
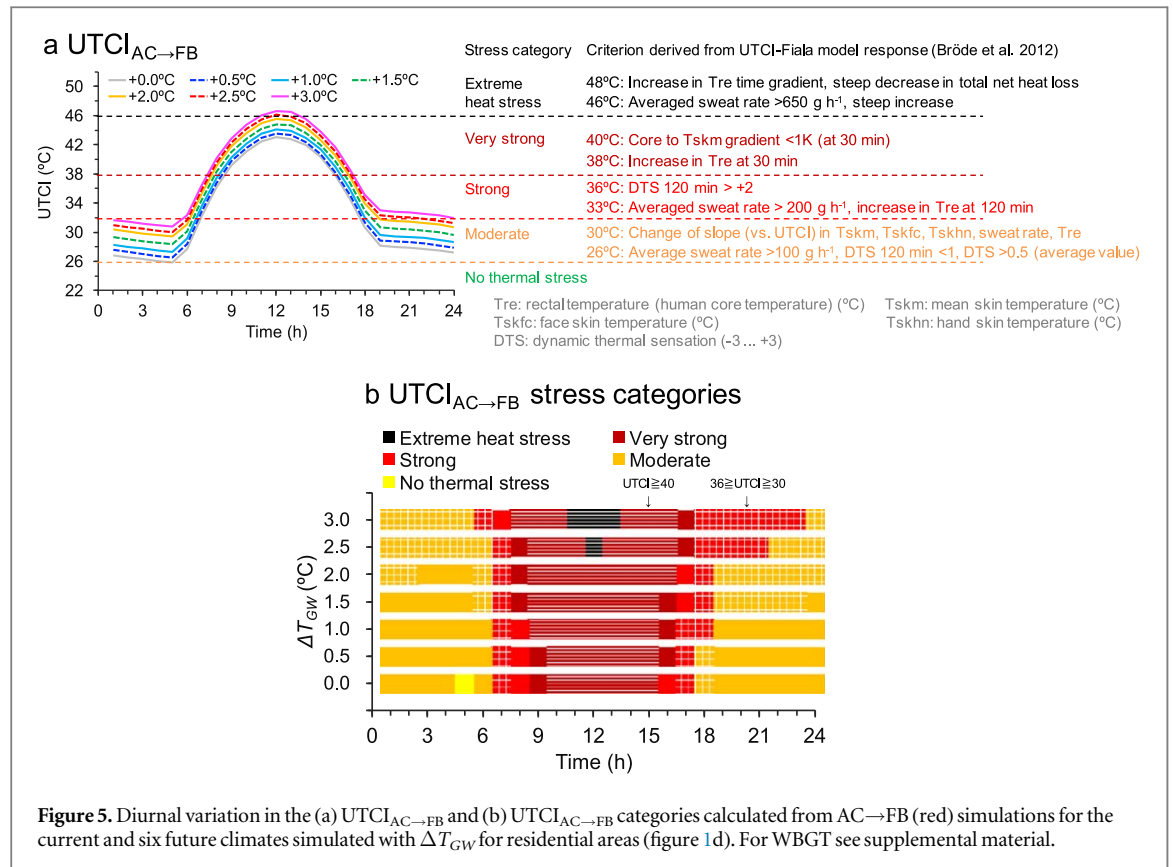
Figure 4. Eleven-year (2000–2010) mean UTCI for August at (a)–(g) 05:00 and (h)–(n) 12:00 under different climates: (a), (h) current and ΔT_{GW} (b), (i) +0.5 °C; (c), (j) +1.0 °C; (d), (k) +1.5 °C; (e), (l) +2.0 °C; (f), (m) +2.5 °C; and (g), (n) +3.0 °C. All times are local (UTC + 9 h); Japan does not use daylight saving time. For WBGT see supplemental material.

3. Results

The ΔT_{GW} changes the temperature, wind, humidity, and radiation in WRF. In the results, wind speed and T_{mrt} increase a small amount with ΔT_{GW} at night but do not change during the day. Hence, their ΔT_{GW} impact on the UTCI could be small. Relative humidity changes a little from the temperature and specific humidity increases.

3.1. UTCI increase ($\Delta UTCI$) with global warming (ΔT_{GW})

The UTCI is greater in Osaka than in the surrounding land areas at 05:00 under all seven climates (current and six future scenarios, figures 4(a)–(g)), we refer to these as urban heat 'stress' islands. In the current climate, Osaka (white line, figure 4(a)) has moderate heat stress but with greater urban warming (ΔT_{GW}), this area expands to cover the entire plain when $\Delta T_{GW} = +1.5$ °C (figure 4(d)), and extends to the low-mountain area (figure 4(g)) with additional warming. People outdoors in this moderate heat stress area will sweat (sweat rate >100 g h^{-1}) and experience wet skin (Bröde *et al* 2012a). The relatively higher heat stress area is in the coastal parts of Osaka and Kobe (black line, figure 4(g)).

At 12:00, UTCI increases with ΔT_{GW}, and feedback effects of AC are projected (figures 4(h)–(n)), but with inland values expected to be higher than those in the coastal area. Under current climate conditions, the entire area, except the high mountains, experiences very strong heat stress (figure 4(h)). When $\Delta T_{GW} = +1.5$ °C, the mountain area is included in that description (figure 4(k)). Under such conditions, the human body core temperature of people outdoors for 30 min can increase (Bröde *et al* 2012a). When $\Delta T_{GW} = +2.0$ °C, an extreme heat stress area is projected inland from Osaka, covering Kyoto and Nara (black lines, figure 4(l)). When
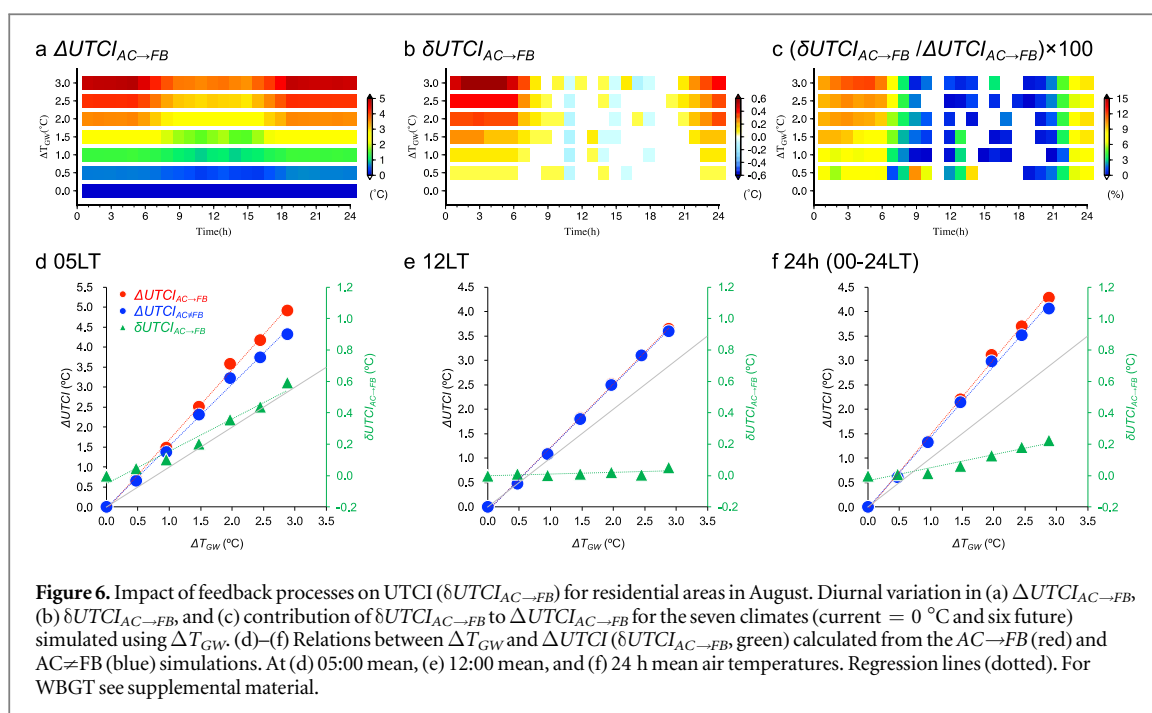
Figure 5. Diurnal variation in the (a) $UTCI_{AC \to FB}$ and (b) $UTCI_{AC \to FB}$ categories calculated from AC→FB (red) simulations for the current and six future climates simulated with ΔT_{GW} for residential areas (figure 1d). For WBGT see supplemental material.

$\Delta T_{GW} = +3.0\ ^\circ$C, it covers most of the plain (figure 4(n)). Under these conditions, people will sweat at more than 650 g h^{-1}, show large increases in their core temperature, and have a lower net heat loss (Bröde *et al* 2012a).

The changes in the diurnal range of UTCI projected for the current and six future temperature scenarios are similar, but the individual mean values of UTCI differ (figure 5(a)). In the current climate, there is 1 h with no thermal stress (~05:00), but this disappears with only a small amount of warming (after $\Delta T_{GW} = +0.5\ ^\circ$C) (yellow, figure 5(b)). The midnight-to-morning period of moderate heat stress remains almost constant with ΔT_{GW}, unlike the evening-to-midnight period, which decreases with ΔT_{GW} from (orange, figure 5(b)). Notably, the latter becomes a strong heat stress (red, figure 5(b)) period once $\Delta T_{GW} = +2.0\ ^\circ$C. Under $\Delta T_{GW} = +3.0\ ^\circ$C, the period is projected to persist until midnight. The very strong heat stress daytime period increases with ΔT_{GW} (dark red, figure 5(b)). Under $\Delta T_{GW} = +2.5\ ^\circ$C, extreme heat stress conditions are expected by 12:00, persisting longer with ΔT_{GW} (black in figure 5(b)).

3.2. Impact of AC induced feedback on UTCI ($\delta UTCI_{AC \to FB}$)

The feedback effects of air-conditioning on UTCI ($\delta UTCI_{AC \to FB}$) are much greater at night than during the day in residential areas (figure 6(b)), with changing climate expected to have greater influence in the early morning. The size of this feedback increases roughly linearly with the global temperature increases (figures 6(d), (e)). At 05:00, $\delta UTCI_{AC \to FB}$ increases with ΔT_{GW} (figures 7(a)–(f)) but is smaller in the centre of Osaka (figures 7(b)–(f)). However, at 12:00, $\delta UTCI_{AC \to FB}$ does not change with ΔT_{GW} (figures 6(b), (e)). These differences are probably caused by the difference in mixed layer depth, as Takane *et al* (2019) proposed. In the middle of the day, $Q_{F,AC}$ is large, but the deeper mixed layer reduces its impact on UTCI. At night, although $Q_{F,AC}$ is smaller, the mixed layer is much smaller. Consequently, $Q_{F,AC}$ enhances the mixed depth, and there is a greater impact on UTCI.

Increased temperature from the nocturnal feedback causes an increase in T_{mrt} which could contribute to an UTCI increase. The contribution of $\delta UTCI_{AC \to FB}$ to $\Delta UTCI_{AC \to FB}$ (figure 6(c)) is influenced by the $\delta UTCI_{AC \to FB}$ diurnal pattern (figure 6(b)), with the contribution for the night-to-morning period being larger than that in the daytime. The early morning contribution is about 12% when $\Delta T_{GW} = +3.0\ ^\circ$C. These results suggest that one reason for the relatively higher $\Delta UTCI_{AC \to FB}$ at night (figure 6(a)) is the feedback process. The spatial distribution of the contribution of $\delta UTCI_{AC \to FB}$ to $\Delta UTCI_{AC \to FB}$ (figures 7(g)–(i)) is similar to that of $\delta UTCI_{AC \to FB}$ (figures 7(a)–(f)).

Figure 6. Impact of feedback processes on UTCI ($\delta UTCI_{AC \rightarrow FB}$) for residential areas in August. Diurnal variation in (a) $\Delta UTCI_{AC \rightarrow FB}$, (b) $\delta UTCI_{AC \rightarrow FB}$, and (c) contribution of $\delta UTCI_{AC \rightarrow FB}$ to $\Delta UTCI_{AC \rightarrow FB}$ for the seven climates (current $= 0$ °C and six future) simulated using ΔT_{GW}. (d)–(f) Relations between ΔT_{GW} and $\Delta UTCI$ ($\delta UTCI_{AC \rightarrow FB}$, green) calculated from the $AC \rightarrow FB$ (red) and $AC \neq FB$ (blue) simulations. At (d) 05:00 mean, (e) 12:00 mean, and (f) 24 h mean air temperatures. Regression lines (dotted). For WBGT see supplemental material.

4. Discussion

4.1. Hot and cold summers: consideration of heat waves

Differences in UTCI diurnal pattern are expected in a warmer summer climate. From the 11 current summers, we identify a hot (2010, figure 8(a)) and cold (2003, figure 8(c)) summer to compare to the mean (figure 8(b)). The hot and cold summer temperatures are 30.5 °C and 28.3 °C, respectively, or 1.52 °C warmer and 0.68 °C cooler than the 11-year mean. The August 2010 temperature roughly corresponds to the conditions expected when $\Delta T_{GW} = +1.5$ °C (i.e. above the summer mean). These individual summers were selected for each of the future climates for comparison (figure 8).

The patterns of the hot summer (figure 8(a)) diurnal UTCI classes when $\Delta T_{GW} = 0.0$ to $+2.0$ °C are similar to the mean for $\Delta T_{GW} = +1.0$ to $+3.0$ °C (figure 8(b), solid blue rectangle). Similarly, the cold summer (figure 8(c)) UTCI patterns for $\Delta T_{GW} = +0.5$ to $+3.0$ °C are similar to the mean for $\Delta T_{GW} = 0.0$ to $+2.5$ °C (figure 8(b), solid green rectangle). Therefore, the hot summer UTCI patterns for $\Delta T_{GW} = +2.5$ and $+3.0$ °C provide some insight into more extreme mean climate (e.g. $\Delta T_{GW} = +3.5$ and $+4.0$ °C, dashed blue rectangle). Similarly, the cold summer UTCI pattern at $\Delta T_{GW} = 0.0$ °C reflects the impact of an urban heat island mitigation of about 0.5 °C using current techniques for the current climate ($\Delta T_{GW} = 0.0$ °C, dashed green rectangle). Comparing these, the need to respond to or modify the future UTCI pattern caused by global warming and urban heat island mitigation techniques can be considered, in addition to the inter-annual summer variability within ΔT_{GW}.
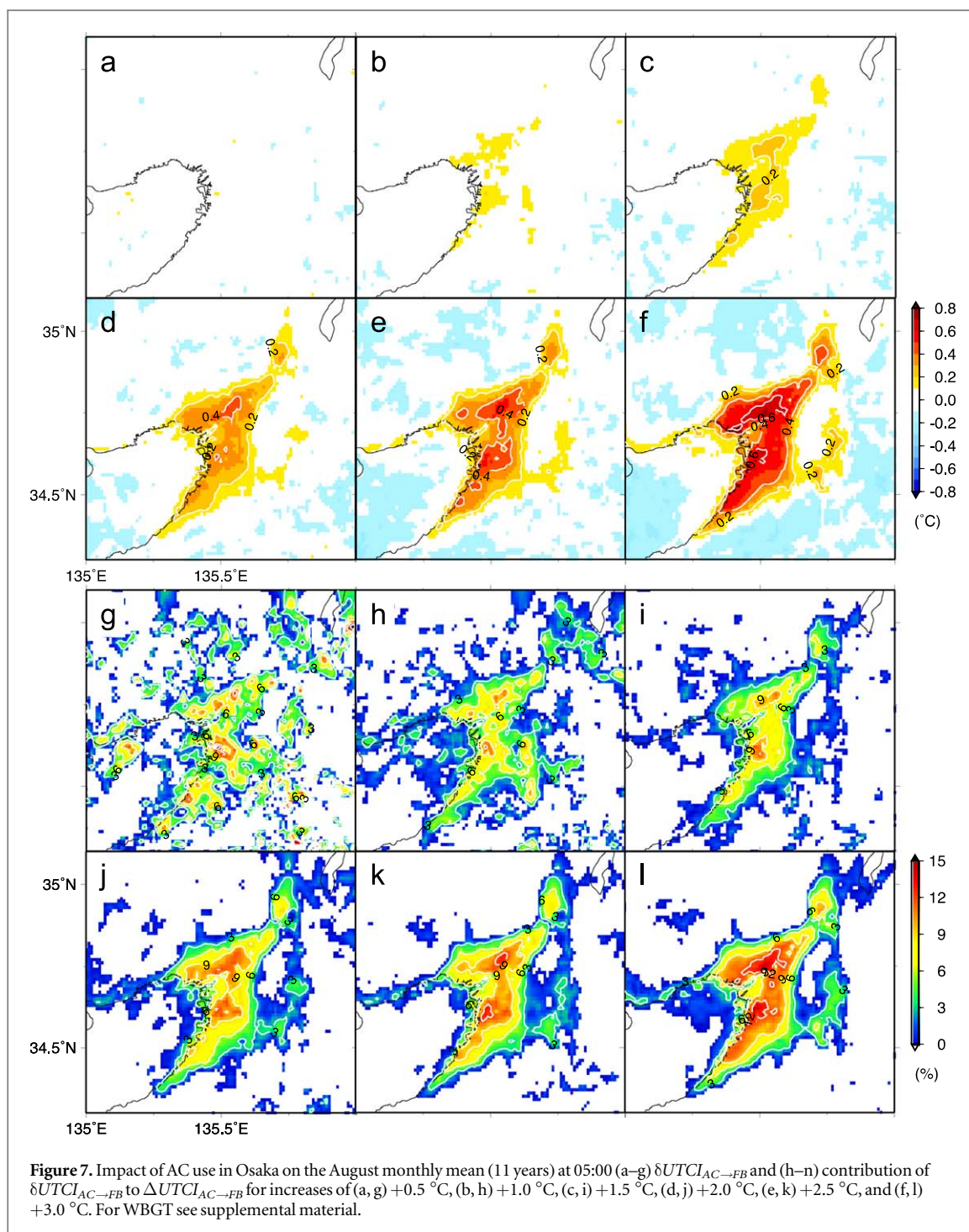
The August 2013 and July 2018 Japanese heat waves had monthly mean temperatures in Osaka of 30.0 °C (0.99 °C warmer than the 11-year August mean (2000–2010)) and 29.5 °C (0.45 °C warmer), roughly corresponding to $\Delta T_{GW} = 1.0$ and 0.5 °C, respectively (figure 8(b), dashed pink rectangle). The observed diurnal UTCI class patterns for the two heat waves (figure 8(d)) are similar to those of $\Delta T_{GW} = 1.0$ and 0.5 °C (figure 8(b), dashed pink rectangle).

This approach provides a rough estimate of the future climate UTCI for specific heat and cold waves using past hot and cold summers for comparison.

4.2. Heat stress metrics

Two heat-related physiological responses, sweat production and human body core temperature, increase non-linearly once UTCI exceeds 40 °C (very strong and extreme heat stresses), whereas human thermal sensation does not (Bröde *et al* 2012a). In Osaka, daytime UTCI is projected to exceed 40 °C during current and future climates (figure 5(b), table S2). The impact of the feedback on core temperature is estimated to be less than 0.05 °C (not shown) and is regarded as not significant in terms of heat stroke vulnerability.

As human thermal sensation does not continue to change with an increase in UTCI, there is the danger that people will not feel the increasing heat stroke vulnerability. The critical UTCI range is 30 °C–36 °C (moderate to
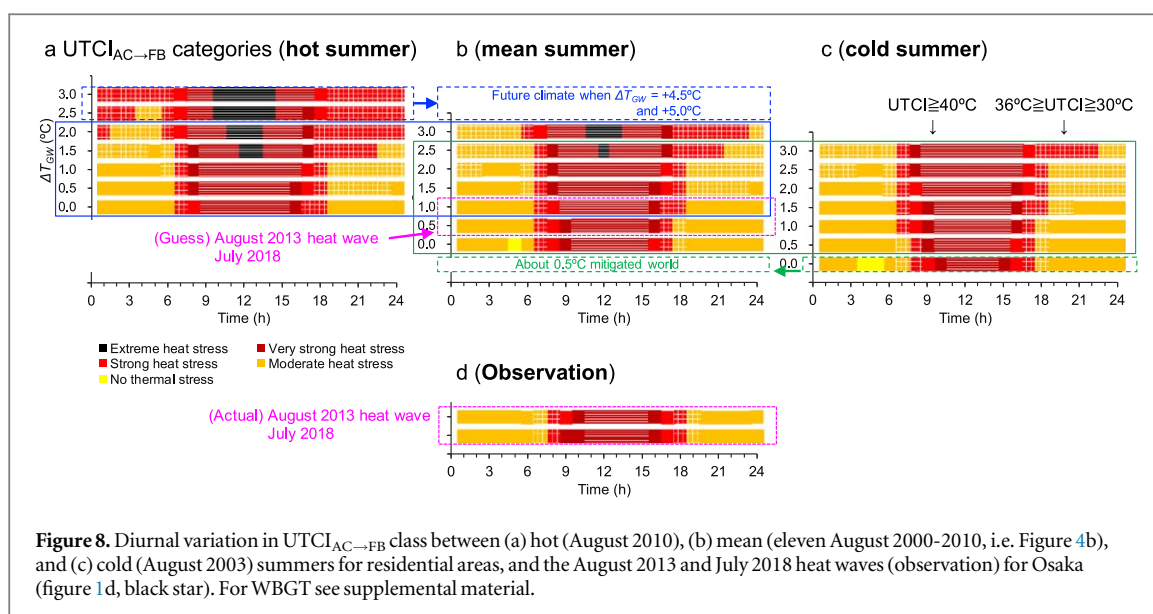
Figure 7. Impact of AC use in Osaka on the August monthly mean (11 years) at 05:00 (a–g) $\delta UTCI_{AC \rightarrow FB}$ and (h–n) contribution of $\delta UTCI_{AC \rightarrow FB}$ to $\Delta UTCI_{AC \rightarrow FB}$ for increases of (a, g) +0.5 °C, (b, h) +1.0 °C, (c, i) +1.5 °C, (d, j) +2.0 °C, (e, k) +2.5 °C, and (f, l) +3.0 °C. For WBGT see supplemental material.

strong, Bröde *et al* 2012a), suggesting that awareness of the changes from early evening to morning (figure 5(b), table S2) is critical for heat stroke prevention.

The diurnal variation and spatial patterns of UTCI in Osaka (figures 4–7) are similar to WBGT (Supplementary material), as others have noted (Zare *et al* 2018). This suggests the widely available WBGT maps can be roughly used to infer probable UTCI spatial patterns.

As the grid average heat stress metrics calculated in this study do not capture the intra-grid variability (e.g. from shade), the values are more applicable to outdoor workers than to individuals who can seek shade outdoors or go indoors to AC areas.

4.3. Relative impact of the AC feedback and thermal mitigation to heat stress metrics

The impact of the AC feedback ($\delta UTCI_{AC \rightarrow FB}$) simulated when $\Delta T_{GW} = +3.0$ °C reached 0.6 °C for UTCI and 0.4 °C for WBGT (Supplementary Material) with 24-h means 0.23 and 0.15 °C, respectively. These are of similar size to some proposed thermal mitigation strategies. For example, the estimated decreases in UTCI with

Figure 8. Diurnal variation in $UTCI_{AC \to FB}$ class between (a) hot (August 2010), (b) mean (eleven August 2000-2010, i.e. Figure 4b), and (c) cold (August 2003) summers for residential areas, and the August 2013 and July 2018 heat waves (observation) for Osaka (figure 1d, black star). For WBGT see supplemental material.

different strategies for residential Lyon in summer include 0.2 °C–0.4 °C from water aspersion and 0.4 °C–0.7 °C from vegetation (Morille and Musy 2017). Similarly, facade greening (roofs and walls) are estimated to be able decrease the August daytime maximum WBGT by 0.02 °C–0.03 °C, and the relocation of AC heat release from walls to roofs by 0.03 °C–0.06 °C for the 23 wards of Tokyo (Ohashi *et al* 2016). However, our estimated feedbacks would negate the mitigation benefits from these techniques in future climates, especially where AC use is high.

4.4. Future work
Our results the impact of AC on future temperatures suggest is of sufficient importance that future work is warranted:

(1) Here heat stress metrics are calculated at 1 km scale but more detailed micro-scale variations (e.g. accounting for shadow patterns from building and vegetation such as by SOLWEIG Lindberg *et al* 2008) would allow human behaviour (e.g. movement) to be considered (e.g. Honjo *et al* 2018).

(2) Our estimates of the feedback on heat stress metrics may be low as a constant coefficient of performance (COP) is assumed. A variable COP would be more realistic and should be considered in future studies (e.g. CM-BEM Kikegawa *et al* 2014; TEB+BEM Bueno *et al* 2012; UCLEM Lipson *et al* 2018, 2019).

(3) Our focus has been on building energy emissions from AC but Q_F sources from traffic, cooling towers, non-work day energy use variation, and electric and gas AC in office areas should all be considered.

(4) Analysis of other regions using the same methods to generalise the feedback impact, as the impacts may depend on climate, building type/materials, AC performance and human behaviours (e.g. how AC is used).

(5) The UTCI heat stress and physiological response is based on Europeans. Other regions and conditions need to be studied: e.g. Asian city residents.

5. Conclusions

Effects of GHG-induced global warming on heat stress are considered by analysing RCM (with urban canopy and building energy models) dynamically downscaled simulatons for current and six future climate scenarios (global warming: ΔT_{GW}). For the latter, CMIP5 global climate model (GCM) simulations with the highest IPCC greenhouse gas emissions scenario (RCP 8.5) are used. Two heat stress indices are calculated for Osaka during August, when air conditioning (AC) use (hence energy consumption) is greatest. From this we conclude:

(i) Heat stress (e.g. UTCI) increases with ΔT_{GW} and with AC feedback. At night, an urban heat stress island (i.e. higher UTCI in the urban area compared with the surroundings) is simulated in Osaka for the current and six future climates. In the current climate, only 1 h of no thermal stress occurs near 05:00, but this disappears with $\Delta T_{GW} = +0.5$ °C and warmer climates. Moderate heat stress extends across the entire Osaka plain

when $\Delta T_{GW} = +1.5\,°C$. People outside under these conditions begin to sweat, and their skin wetness increases.

(ii) Daytime UTCI tends to be greater inland than in coastal areas. An extreme heat stress area appears when $\Delta T_{GW} = +2.0\,°C$ inland, affecting Kyoto and Nara. This extends over most of the plain when $\Delta T_{GW} = +3.0\,°C$. These are dangerous conditions for people outdoors, as they may experience large increases in sweating and human body core temperature, and lose the ability to shed heat unless they seek opportunities to reduce heat stress (e.g. shade outdoors, AC indoors).

(iii) The impact of AC-induced feedback on UTCI increases ($\delta UTCI_{AC \to FB}$) roughly linearly with ΔT_{GW}. At $\Delta T_{GW} = +3.0\,°C$, this reaches $0.6\,°C$ (12% of UTCI increase). This size is comparable to the suggested benefits of thermal mitigation techniques reported in the literature. Hence, the feedback is significant and could potentially cancel other mitigation benefits in the future, especially where AC use is large. This feedback must not be neglected in future urban climate projections.

(iv) UTCI and WBGT, two independent heat stress metrics, have similar diurnal variation and spatial patterns. As the latter is the official Japanese metric, it may be possible to roughly estimate diurnal variations in UTCI from existing maps of WBGT.

Acknowledgments

ORCID iDs

Yuya Takane ⬤ https://orcid.org/0000-0002-6259-2748
Yukitaka Ohashi ⬤ https://orcid.org/0000-0003-0257-828X
C Sue B Grimmond ⬤ https://orcid.org/0000-0002-3166-9415
Masayuki Hara ⬤ https://orcid.org/0000-0002-7012-4581
Yukihiro Kikegawa ⬤ https://orcid.org/0000-0002-5225-653X

References

Adachi S A, Kimura F, Kusaka H, Inoue T and Ueda H 2012 Comparison of the impact of global climate changes and urbanization on summertime future climate in the Tokyo metropolitan area *Journal of Applied Meteorology and Climatology* **51** 1441–54

Altinsoy H and Yildirim H A 2014 Labor productivity losses over western Turkey in the twenty-first century as a result of alteration in WBGT *International Journal of Biometeorology* **59** 463–71

Argüeso D, Evans J P, Pitman A J and Di Luca A 2015 Effects of city expansion on heat stress under climate change conditions *PLoS One* **10** e0117066

Ashie Y, Vu Thanh C and Asaeda T 1999 Building canopy model for the analysis of urban climate *Journal of Wind Engineering & Industrial Aerodynamics* **81** 237–48

Błażejczyk K, Epstein Y, Jendritzky G, Staiger H and Tinz B 2012 Comparison of UTCI to selected thermal indices *Int. J. Biometeorol.* **56** 515–35

Błażejczyk K, Jendritzky G, Bröde P *et al* 2013 An introduction to the universal Thermal Climate Index (UTCI) *Geographia Polonica* **86** 5–10

Błażejczyk K, Kuchcik M, Błażejczyk A, Milewski P and Szmyd J 2014 Assessment of urban thermal stress by UTCI—experimental and modelling studies: an example from Poland *Die Journal of the Geographical Society of Berlin* **145** 16–33 (https://www.die-erde.org/index.php/die-erde/article/view/98)

Bröde P, Fiala D, Błażejczyk K, Holmér I, Jendritzky G, Kampmann B, Tinz B and Havenith G 2012a Deriving the operational procedure for the Unversal Thermal Climate Index (UTCI) *Int. J. Biometeorol.* **56** 481–94

Bröde P, Krüger L E, Rossi A F and Fiala D 2012b Predicting urban outdoor thermal comfort by the universal Thermal Climate Index (UTCI)—a case study in southern Brazil *Int. J. Biometeorol.* **56** 471–80

Bruyère C L, Done J M, Holland G J and Fredrick S 2014 Bias corrections of global models for regional climate simulations of high-impact weather *Clim. Dyn.* **43** 1847–56

Bruyère C L, Monaghan A J, Steinhoff D F and Yates D 2015 Bias-corrected CMIP5 CESM data in WRF/MPAS intermediate file format *TN-515 + STR, NCAR* **1** p 27 (https://opensky.ucar.edu/islandora/object/technotes:527) TN-515+STR, NCAR

Bueno B, Pigeon G, Norford L K, Zibouche K and Marchadier C 2012 Development and evaluation of a building energy model integrated in the TEB scheme *Geoscientific Model Development* **5** 433–48

Coffel E D, Horton R M and Sherbinin A D 2018 Temperature- and humidity-based projections of a rapid rise in global heat stress exposure during the 21st century *Environ. Res. Lett.* **13** 014001

Conlon K, Monaghan A, Hayden M and Wilhelmi O 2016 Potential impacts of future warming and land use changes on intra-urban heat exposure in Houston, Texas *PLoS One* **11** e0148890

Chen F and Dudhia J 2001 Coupling an advanced land–surface/hydrology model with the Penn State/NCAR MM5 modeling system. Part I: Model description and implementation *Mon. Weather Rev.* **129** 569–85

Darmanto N S, Varquez A C G, Kawano N and Kanda M 2019 Future urban climate projection in a tropical megacity based on global climate change and local urbanization scenarios *Urban Climate* **29** 100482

Delworth T L, Mahlman J D and Knutson T R 1999 Changes in heat index associated with CO_2-induced global warming *Clim. Change* **43** 369–86

Diffenbaugh N S, Pal J S, Giorgi F and Gao X 2007 Heat stress intensification in the Mediterranean climate change hotspot *Geophys. Res. Lett.* **34** L11706

Doan V Q and Kusaka H 2018 Projections of urban climate in the 2050s in a fast-growing city in Southeast Asia: the greater Ho Chi Minh City metropolitan area, Vietnam *Int. J. Climatol.* **38** 4155–71

Doan V Q, Kusaka H and Ho Q-B 2016 Impact of future urbanization on temperature and thermal comfort index in a developing tropical city: Ho Chi Minh City *Urban Climate* **17** 20–31

Donner L J *et al* 2011 The dynamical core, physical parameterizations, and basic simulation characteristics of the atmospheric component of the GFDL global coupled model CM3 *J. Clim.* **24** 3484–518

Dudhia J 1989 Numerical study of convection observed during the winter monsoon experiment using a mesoscale two-dimensional model *J. Atmos. Sci.* **46** 3077–107

Fiala D, Havenith G, Bröde P, Kampmann B and Jendritzky G 2012 UTCI—Fiala multi-node model of human heat transfer and temperature regulation *Int. J. Biometeorol.* **56** 429–41

Fiala D, Psikuta A, Jendritzky G, Paulke S, Nelson D A, van Marken Lichtenbelt W D and Frijns A J H 2010 Physiological modeling for technical, clinical and research applications *Frontiers in Bioscience* **S2** 939–968 (https://www.bioscience.org/2010/v2s/af/112/fulltext.htm)

Fischer E M, Oleson K W and Lawrence D M 2012 Contrasting urban and rural heat stress responses to climate change *Geophys. Res. Lett.* **39** L03705

Gent P R *et al* 2011 The community climate system model version 4 *Journal of Climate* **24** 4973–91

Ginzhurg A S and Demchenko P F 2019 Anthropogenic meso-meteorological feedbacks: A review of a recent research *Izvestiya, Atmospheric and Oceanic Physics* **55** 573–90

Grossman-Clarke S, Schubert S and Fenner D 2016 Urban effects on summertime air temperature in Germany under climate change *Int. J. Climatol.* **37** 905–17

Hamdi R, Van de Vyver H, De Troch R and Termonia P 2014 Assessment of three dynamical urban climate downscaling methods: Brussels's future urban heat island under an A1B emission scenario *Int. J. Climatol.* **34** 978–99

Hara M, Yoshikane T, Kawase H and Kimura F 2008 Estimation of the impact of global warming on snow depth in Japan by the pseudo-global warming method *Hydrological Research Letters* **2** 61–4

Hong S-Y, Dudhia J and Chen S-H 2004 A revised approach to ice microphysical processes for the bulk parameterization of clouds and precipitation *Mon. Weather Rev.* **132** 103–20

Honjo T, Seo Y, Yamasaki Y, Tsunematsu N, Yokoyama H, Yamato H and Mikami T 2018 Thermal comfort along the marathon course of the 2020 Tokyo Olympics *Int. J. Biometeorol.* **62** 1407–19

Iacono M J, Delamere J S, Mlawer E J, Shephard M W, Clough S A and Collins W D 2008 Radiative forcing by long—lived greenhouse gases: calculations with the AER radiative transfer models *Journal of Geophysical Research* **113** D13103

IPCC 2013 Climate Change 2013: The Physical Science Basis. Contribution of Working Group I to the Fifth *Assessment Report of the Intergovernmental Panel on Climate Change* ed T F Stocker *et al* (Cambridge, United Kingdom and New York, NY, USA: Cambridge University Press) p 1535

IPCC Climate Change 2014: Impacts, Adaptation, and Vulnerability. Part A: Global and Sectoral Aspects. Contribution of Working Group II to the Fifth *Assessment Report of the Intergovernmental Panel on Climate Change* ed C B Field *et al* 2014 (Eds) (Cambridge, United Kingdom and New York, NY, USA: Cambridge University Press) p 1132

Janjic Z 1994 The Step—Mountain Eta Coordinate Model: further developments of the convection, viscous sublayer, and turbulence closure schemes *Mon. Weather Rev.* **122** 927–45

Janjic Z 2002 Nonsingular implementation of the Mellor–Yamada level 2.5 scheme in the NCEP Meso model *NCEP Office Note* **436** 61

Kalnay E *et al* 1996 The NCEP/NCAR 40–year reanalysis project *Bull. Am. Meteorol. Soc.* **77** 437–71

Kawase H, Yoshikane T, Hara M, Ailikun B, Kimura F and Yasunari T 2008 Downscaling of the climatic change in the Mei-yu rainband in East Asia by a pseudo climate simulation method *SOLA* **4** 73–6

Kawase H, Yoshikane T, Hara M, Kimura F, Yasunari T, Ailikun B, Ueda H and Inoue T 2009 Intermodel variability of future changes in the Baiu rainband estimated by the pseudo global warming downscaling method *J. Geophys. Res.* **114** D24110

Kikegawa Y, Genchi Y, Yoshikado Y and Kondo H 2003 Development of a numerical simulation system for comprehensive assessments of urban warming countermeasures including their impacts upon the urban buildings' energy demands *Appl. Energy* **76** 449–66

Kikegawa Y, Tanaka A, Ohashi Y, Ihara T and Shigeta Y 2014 Observed and simulated sensitivities of summertime urban surface air temperatures to anthropogenic heat in downtown areas of two Japanese Major Cities, Tokyo and Osaka *Theor. Appl. Climatol.* **117** 175–93

Kikumoto H, Ooka R and Arima Y 2016 A study of urban thermal environment in Tokyo in summer of the 2030s under influence of global warming *Energy Build.* **114** 54–61

Kimura F and Kitoh A 2007 Downscaling by pseudo global warming method *The Final Report of the ICCAP* (Kyoto, Japan: Research Institute for Humanity and Nature)

Kinouchi T 2001 A study on thermal indices for the outdoor environment *Tenki* **48** 661–71 (in Japanese with English abstract)

Krayenhoff E S, Moustaoui M, Broadbent A M, Gupta V and Georgescu M 2018 Diurnal interaction between urban expansion, climate change and adaptation in US cities *Nat. Clim. Change* **8** 1097–103

Kurihara Y, Sakurai T and Kuragano T 2006 Global daily sea surface temperature analysis using data from satellite microwave radiometer, satellite infrared radiometer and *in situ* observation (in Japanese) *Weather Service Bulletin* **73** S1–18

Kusaka H, Hara M and Takane Y 2012 Urban climate projection by the WRF model at 3-km grid increment: dynamical downscaling and predicting heat stress in the 2070's August for Tokyo, Osaka, and Nagoya *Journal of Meteorological Society of Japan* **90B** 47–64

Kusaka H, Suzuki-Parker A, Aoyagi T, Adachi S A and Yamagata Y 2016 Assessment of RCM and urban scenarios uncertainties in the climate projections for August in the 2050s in Tokyo *Clim. Change* **137** 427–38

Li C, Zhou J, Cao Y, Zhong J, Liu Y, Kang C and Tan Y 2014 Interaction between urban microclimate and electric air-conditioning energy consumption during high-temperature seasons *Appl. Energy* **117** 149–56

Lindberg F, Thorsson S and Holmer B 2008 SOLWEIG 1.0—Modelling spatial variations of 3D radiant fluxes and mean radiant temperature in complex urban settings *Int. J. Biometeorol.* **52** 697–713

Lipson M J, Thatcher M, Hart M A and Pitman A 2018 A building energy demand and urban land surface model *Q. J. R. Meteorolog. Soc.* **144** 1572–90

Lipson M J, Thatcher M, Hart M A and Pitman A 2019 Climate change impact on energy demand in building-urban-atmosphere simulations through the 21st century *Environ. Res. Lett.* **14** 125014

Martilli A, Clappier A and Rotach M W 2002 An urban surface exchange parameterization for mesoscale models *Boundary Layer Meteorol.* **104** 261–304

Meehl G A *et al* 2013 Climate change projections in CESM1(CAM5) compared to CCSM4 *J. Clim.* **26** 6287–308

Mellor G C and Yamada T 1982 Development of a turbulence closure model for geophysical fluid problems *Rev. Geophys. Space Phys.* **20** 851–75

Ministry of Internal Affairs and Communications, Japan 2018 (https://www.fdma.go.jp/disaster/heatstroke/item/heatstroke003_houdou04.pdf)

Mora C *et al* 2017 Global risk of deadly heat *Nat. Clim. Change* **7** 501–6

Morille B and Musy M 2017 Comparison of the impact of three climate adaptation strategies on summer thermal comfort—case study in Lyon *France Procedia Environmental Science* **38** 619–26

Nikkei 2018 (https://www.nikkei.com/article/DGXMZO33291910T20C18A7EA1000/)

Ohashi Y, Ihara T, Kikegawa Y and Sugiyama N 2016 Numerical simulations of influence of heat island countermeasures on outdoor human heat stress in the 23 wards of Tokyo, Japan *Energy Build.* **114** 104–11

Ohashi Y, Katsuta T, Tani H, Okabayashi T, Miyahara S and Miyashita R 2018 Human cold stress of strong local-wind 'Hijikawa-arashi' in Japan, based on the UTCI index and thermo-physiological responses *Int. J. Biometeorol.* **62** 1241–50

Ohashi Y, Kikegawa Y, Ihara T and Sugiyama N 2014 Numerical simulations of outdoor heat stress index and heat disorder risk in the 23 wards of Tokyo *Journal of Applied Meteorology and Climatology* **53** 583–97

Okada M and Kusaka H 2013 Proposal of a new equation to estimate globe temperature in an urban park environment *Journal of Agricultural Meteorology* **69** 23–32

Okada M, Okada M and Kusaka H 2013 Parameter adjustment and application to an extension area of Okada and Kusaka's formula for the black globe temperature *Journal of Heat Island Institute International* **8** 13–21 (in Japanese with English abstract)

Oleson K W, Monaghan A, Wilhelmi O, Barlage M, Brunsell N, Feddema J, Hu L and Steinhoff D F 2015 Interactions between urbanization, heat stress, and climate change *Clim. Change* **129** 525–41

Provençal S, Bergeron O, Leduc R and Barrette N 2016 Thermal comfort in Quebec City, Canada: sensitivity analysis of the UTCI and other popular thermal comfort indices in a mid-latitude continental city *Int. J. Biometeorol.* **60** 591–603

Rasmussen R *et al* 2011 High-resolution coupled climate runoff simulations of seasonal snowfall over Colorado: a process study of current and warmer climate *J. Clim.* **24** 3015–48

Sailor D J 2011 A review of methods for estimating anthropogenic heat and moisture emissions in the urban environment *Int. J. Climatol.* **31** 189–99

Salamanca F, Georgescu M, Mahalov A, Moustaoui M and Wang M 2014 Anthropogenic heating of the urban environment due to air conditioning *Journal of Geophysical Research Atmosphere* **119** 5949–65

Salamanca F, Krpo A, Martilli A and Clappier A 2010 A new building energy model coupled with an urban canopy parameterization for urban climate simulations—part I. formulation, verification, and sensitivity analysis of the model *Theor. Appl. Climatol.* **99** 331–44

Salamanca F and Martilli A 2010 A new building energy model coupled with an urban canopy parameterization for urban climate simulations—part II. Validation with one dimension off–line simulations *Theor. Appl. Climatol.* **99** 345–56

Sato T, Kimura F and Kitoh A 2007 Projection of global warming onto regional precipitation over Mongolia using a regional climate model *J. Hydrol.* **333** 144–54

Schreier S, Suomi I, Bröde P, Formayer H, Rieder E H, Nadeem I, Jendritzky G, Batchvarova E and Weihs P 2013 The uncertainty of UTCI due to uncertainties in the determination of radiation fluxes derived from numerical weather prediction and regional climate model simulations *Int. J. Biometeorol.* **57** 207–23

Skamarock W C, Klemp J B, Dudhia J, Gill D O, Barker D M, Duda M G, Huang X–Y, Wang W and Powers J G A 2008 description of the Advanced Research WRF version 3. NCAR TechNote NCAR/TN–4751STRp 113 Available online at: http://mmm.ucar.edu/wrf/users/docs/arw_v3.pdf

Suzuki-Parker A and Kusaka H 2015 Future projection of thermal environment in Japan using WBGT *Japanese Journal of Biometeorology* **52** 59–72 (in Japanese with English abstract)

Suzuki-Parker A and Kusaka H 2016 Future projections of labor hours based on WBGT for Tokyo and Osaka, Japan, using multi-period ensemble dynamical downscale simulations *Int. J. Biometeorol.* **60** 307–10

Takane Y, Aoki S, Kikegawa Y, Yamakawa Y, Hara M, Kondo H and Iizuka S 2015 Future projection of electricity demand and thermal comfort for August in Nagoya city by WRF–CM–BEM *Journal of Environmental Engineering, AIJ* **80** 973–83

Takane Y, Kikegawa Y, Hara M and Grimmond C S B 2019 Urban warming and future air-conditioning use in an Asian megacity: Importance of positive feedback *npj Climate and Atmospheric Science* **2** 39

Takane Y, Kikegawa Y, Hara M, Ihara T, Ohashi Y, Adachi S A, Kondo H, Yamaguchi K and Kaneyasu N 2017 A climatological validation of urban air temperature and electricity demand simulated by a regional climate model coupled with an urban canopy model and a building energy model in an Asian mega city *Int. J. Climatol.* **37** 1035–52

Takane Y, Ohashi Y, Kusaka H, Shigeta Y and Kikegawa Y 2013 Effects of synoptic-scale wind under the typical summer pressure pattern on the mesoscale high-temperature events in the Osaka and Kyoto urban areas by the WRF model *Journal of Applied Meteorology and Climatology* **52** 1764–78

Takaya A, Morioka Y and Behera S K 2014 Role of climate variability in the heatstroke death rates of Kanto region in Japan *Sci. Rep.* **4** 5655

Taylor K E, Stouffer R J and Meehl G A 2012 An overview of CMIP5 and the experiment design *Bull. Am. Meteorol. Soc.* **93** 485–98

Tewari M, Yang J, Kusaka H, Salamanca F P, Watson C and Treinish L 2019 Interaction of urban heat islands and heat waves under current and future climate conditions and their mitigation using green and cool roofs in New York City and Phoenix, Arizona *Environ. Res. Lett.* **14** 034002

United Nations 2014 Department of Economic and Social Affairs, Population Division, World Urbanization Prospects: the 2014 Revision, Highlights (ST/ESA/SER.A/352) (https://population.un.org/wup/Publications/Files/WUP2014-Highlights.pdf)

Volodin E M, Diansky N A and Gusev A V 2010 Simulating present-day climate with the INMCM4.0 coupled model of the atmospheric and oceanic general circulations *Izvestia, Atmospheric and Oceanic Physics* **46** 414–31

Willett K M and Sherwood S 2012 Exceedance of heat index thresholds for 15 regions under a warming climate using the wet-bulb globe temperature *Int. J. Climatol.* **32** 161–77

Xu Z and Yang X-L 2012 An improved dynamical downscaling method with GCM bias corrections and its validation with 30 years of climate simulations *J. Clim.* **25** 6271–86

Yaglou C P and Minard C D 1957 Controle of heat casualties at military traning centers *Amer. Med. Assoc. Arch. Ind. Health* **16** 302–16

Yamamoto M, Kasai M, Okaze T, Hanaoka K and Mochida A 2018 Analysis of climatic factors leading to future summer heatstroke risk changes in Tokyo and Sendai based on dynamical downscaling of pseudo global warming data using WRF *Journal of Wind Engineering & Industrial Aerodynamics* **183** 187–97

Yang L, Niyogi D, Tewari M, Aliaga D, Chen F, Tian F and Ni G 2016 Contrasting impacts on urban forms on the future thermal environment: example of Beijing metropolitan area *Environ. Res. Lett.* **11** 034018

Yoshikane T, Kimura F, Kawase H and Nozawa T 2012 Verification of the performance of the pseudo-global-warming method for future climate changes during June in East Asia *SOLA* **8** 133–6

Yuge T 1960 Experiments on heat transfer from sphere including combined natural and forced convection *Journal of Heat Transfer* **C82** 214–20

Zare S, Hasheminejad N, Shirvan H E, Hemmatjo R, Sarebanzadeh K and Ahmadi S 2018 Comparing universal Thermal Climate Index (UTCI) with selected thermal indices/environmental parameters during 12 months of the year *Weather and Climate Extremes* **19** 49–57

Zhao L, Lee X, Smith R B and Oleson K 2014 Strong contribution of local background climate to urban heat island *Nature* **511** 216